Proc. Natl. Acad. Sci. USA
Vol. 91, pp. 8950–8954, September 1994
Neurobiology

Cyanotriphenylborate: Subtype-specific blocker of glycine receptor chloride channels

NILS RUNDSTRÖM, VOLKER SCHMIEDEN, HEINRICH BETZ, JOACHIM BORMANN, AND DIETER LANGOSCH

Max-Planck-Institut für Hirnforschung, Deutschordenstrasse 46, D-60528 Frankfurt, Germany

Communicated by Erwin Neher, May 9, 1994

ABSTRACT **The inhibitory glycine receptor is a ligand-gated ion-channel protein existing in different homo- and heterooligomeric isoforms. Here we show that the chloride channel of the recombinant α1-subunit homooligomeric glycine receptor is efficiently blocked by cyanotriphenylborate (CTB) with a concentration effecting 50% inhibition (IC_{50}) of 1.3 μM in the presence of 50 μM glycine. The antagonistic effect of CTB is noncompetitive, use dependent, and more pronounced at positive membrane potentials, suggesting open-channel block. In contrast to α1-subunit receptors, α2-subunit homooligomers are resistant to CTB ($IC_{50} >> 20$ μM). By exchanging the channel-lining transmembrane segment M2 of the α1 polypeptide by that of the α2 polypeptide, we could transfer this resistance to α1 channels, indicating that a single glycine residue at position 254 of the α1 subunit is critical for CTB sensitivity. The blocker did not affect the cation-selective channel of the nicotinic acetylcholine receptor. Thus, CTB may prove useful as a tool to probe the subunit structure of native glycine receptors in mammalian neurons.**

Ligand-gated ion-channel proteins constitute a large superfamily of homologous proteins including the nicotinic acetylcholine receptor (nAcChoR), glycine receptor (GlyR), and γ-aminobutyric acid type A receptor ($GABA_AR$). The pores intrinsic to these proteins are formed by a pentameric arrangement of membrane-spanning subunits. These are built of an N-terminal extracellular domain followed by four predicted transmembrane segments (M1–M4) (reviewed in refs. 1 and 2). Functional analyses of mutagenized receptor subunits have shown segment M2 to line the wall of nAcChoR channels (3–6). Likewise, primary structure variations of M2 segments in GlyR subunits account for the different elementary conductances observed with the recombinant α-subunit homooligomeric and α/β-subunit heterooligomeric GlyR isoforms (7). These functional characteristics were compared to those of glycine-activated conductances in spinal neurons (e.g., refs. 8 and 9) and are consistent with the previously reported exchange of embryonic α2 by adult α1 and β polypeptides *in vivo* (7, 10).

Channel function can be antagonized by blocker molecules in a way that is noncompetitive to agonist binding. Such drugs are thought to inhibit ion permeation by binding to a site within the lumen of an open channel (11). Residues within the M2 segments of different nAcChoR subunits have been photolabeled by blocking agents such as [^{3}H]-triphenylmethylphosphonium bromide (TPMP) (12) or [^{3}H]-chlorpromazine (13) and have been shown to determine the residence time of another blocker, the local anesthetic QX-222 (14). These blockers of the cation-selective nAcChoR channel are amphiphilic organic molecules composed of a lipophilic moiety and a positive charge or a protonatable amine group (reviewed in ref. 11). Previously, we have reported that α homooligomeric but not α/β heterooligomeric GlyRs are inhibited by the uncharged Cl^--channel blocker picrotoxinin. This difference is determined by the primary structure of the respective M2 segments, implying that this segment constitutes the binding site for the blocker (15).

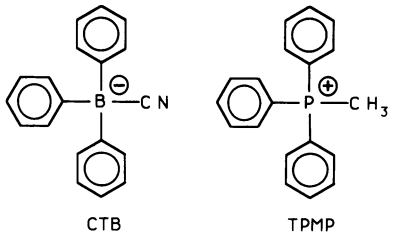

FIG. 1. Molecular structures of the CTB and TPMP ions.

Based on the functional and structural homology of different ligand-gated ion-channel proteins, we assumed that a high-affinity anion-channel blocker should be structurally similar to cation-channel blockers, albeit negatively charged. In an attempt to find organic molecules analogous to the triphenyl structure of TPMP, we identified the cyanotriphenylborate (CTB) anion (Fig. 1). Here we show that this compound blocks the Cl^- channel of certain recombinant GlyR isoforms. Further, for α homooligomers, CTB sensitivity depends on the primary structure of transmembrane segment M2.

MATERIALS AND METHODS

Cell Transfection and Mutagenesis. Human embryonic kidney cells (HEK-293 cells, ATCC CRL 1573) transfected (16) with the human α1-, α2 (17)-, and rat β (18)-subunit cDNAs as well as mutants thereof inserted into the mammalian expression vector pCIS2 (19). The construction of a mutant of the α1 subunit carrying the Gly-254 → Ala mutation, which we call "α1 G254A" (previously denoted α1 G221A), has been described (7). For generating mutant "βB G278A," which carries the mutation Gly-278 → Ala, single-stranded DNA of mutant βB [which is a chimera where the M2 segment of the β subunit is replaced by that of the α1 subunit; see ref. (15)] was used as template for oligonucleotide-directed mutagenesis (Bio-Rad mutagenesis kit) by using 5′-GATGCCCAGAGCTACTCTGGC-3′ as mutagenic oligonucleotide. This generated a construct of the β subunit containing the α2 M2 segment.

Electrophysiological Recording. Whole-cell recordings (20) were obtained from cDNA-transfected HEK-293 cells (7, 15) perfused with a solution containing 137 mM NaCl, 5.4 mM KCl, 1.8 mM $CaCl_2$, 1 mM $MgCl_2$, and 5 mM Hepes (pH 7.4). Patch pipettes contained 120 mM CsCl, 20 mM tetraeth-

The publication costs of this article were defrayed in part by page charge payment. This article must therefore be hereby marked "*advertisement*" in accordance with 18 U.S.C. §1734 solely to indicate this fact.

Abbreviations: CTB, cyanotriphenylborate sodium salt; EC_{50}, 50% effective concentration; nAcChoR, nicotinic acetylcholine receptor; $GABA_AR$, γ-aminobutyric acid type A receptor; GlyR, glycine receptor; HEK-293 cells, human embryonic kidney cells; TPMP, triphenylmethylphosphonium bromide; IC_{50}, concentration effecting half-maximal inhibition; cRNA, complementary RNA.

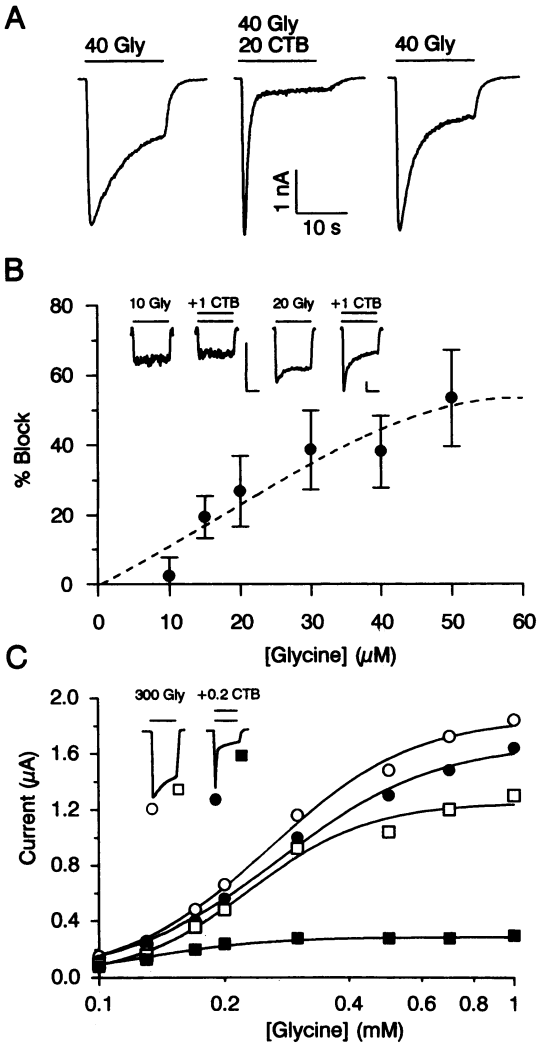

FIG. 2. CTB block of glycine-induced Cl^- currents through α1 homooligomeric GlyR channels expressed in HEK-293 cells. (*A*) Whole-cell recordings at −70-mV transmembrane potential with symmetrical Cl^- concentration (145 mM) at both membrane faces. (*Left*) Application of 40 μM glycine (Gly). (*Center*) Coapplication of 40 μM glycine plus 20 μM CTB. (*Right*) Application of 40 μM glycine after a 2-min wash. The bars indicate periods of drug application (15 s), and the numbers correspond to the drug concentrations in μM. Note the stable peak response, the rapid decline of current in the presence of CTB, and the recovery from block after wash-out of CTB. (*B*) Dependence of CTB efficacy upon glycine concentration. The percentage inhibition of glycine-induced plateau currents by 1 μM CTB is plotted against the glycine concentration coapplied. Data points represent averages (±SD) from 5–14 cells. The dashed line indicates positive correlation of CTB efficacy with glycine concentration. (*Inset*) Two pairs of whole-cell recordings obtained in the absence and presence of 1 μM CTB, where the plateau glycine response was reduced by CTB to 89% of the control at 10 μM glycine (*Left*) and to 57% of the control at 20 μM glycine (*Right*). The membrane potential was held at −70 mV, and drugs were applied for 25 s. The scale bars indicate 10 s (horizontal) and 100 pA (vertical). (*C*) Effect of CTB on the dose–response behavior of glycine-induced currents. The data are from voltage-clamp recordings from *Xenopus* oocytes injected with GlyR α1-subunit cRNA. Curves were constructed from currents measured at −70 mV in response to glycine concentrations ranging from 100 to 1000 μM. Both, peak currents and the responses after a 30-s application period (see bars in *Inset*) were evaluated in the absence and presence of 0.2 μM CTB. The normalized data were fitted with the equation $I = I_{max}C^n/(C^n + EC_{50}^n)$, where I is current, I_{max} is maximal current, C is glycine concentration, and n is the Hill coefficient. From the control curve, EC_{50} values of 258 μM and 270 μM glycine were obtained for the initial peak currents (○) and the residual responses after 30 s (□), respectively. Roughly similar values were obtained in the presence of CTB, the EC_{50} values now being 231 μM and 143 μM for peak currents (●) and the responses after 30 s (■). The Hill coefficients varied from 2.3 to 3.0 between the four curves. (*Inset*) Pair of traces recorded with 300 μM glycine without (*Left*) or with (*Right*) 0.2 μM CTB. Note that, after the 30-s application, the residual response was reduced to *ca.* 26% of the control value by CTB, whereas the initial peak current remained largely constant. It should be noted that the α1 GlyR expressed in oocytes was about 10-fold more sensitive to CTB than in HEK-293 cells (IC_{50} = 0.13 ± 0.1 μM CTB; n = 6 oocytes).

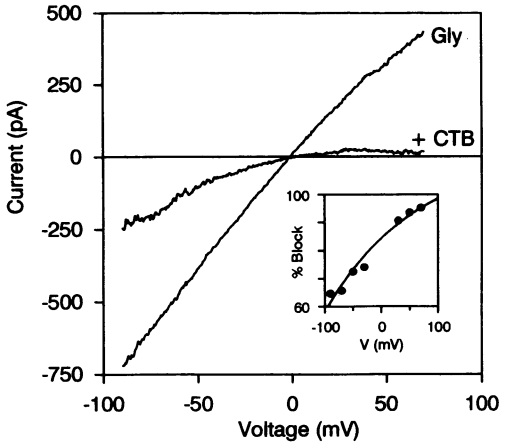

FIG. 3. Voltage dependence of CTB block. *I–V* relationships of glycine-induced whole-cell currents recorded from an α1 cDNA-transfected HEK-293 cell were measured by linearly increasing the membrane potential from −90 to 70 mV (50 mV/s) at symmetrical Cl^- concentrations of 145 mM. Application of 50 μM glycine lead to an almost linear curve, intersecting the voltage axis at *ca.* 0 mV. Upon coapplication of glycine and 1 μM CTB, the *I–V* relationship displayed strong inward rectification. (*Inset*) Percentage block of currents by CTB, plotted as a function of voltage, indicates positive correlation of CTB block with membrane potential.

ylammonium chloride, 1 mM $CaCl_2$, 2 mM $MgCl_2$, 11 mM EGTA, and 10 mM Hepes (pH 7.2). Glycine was applied with a fast-application system (21). When Cl^- was substituted in the pipette solution by another anion, 6 mM Cl^- remained. The data were digitized at 20 Hz or at 1 kHz (in ramp experiments). We corrected for liquid-junction potentials, calculated by the JPCALC program by Peter H. Barry (University of New South Wales, Australia). Whole-cell current–voltage (*I–V*) relations were obtained by linearly increasing (ramping) the membrane potential from −90 to 50 mV (50 mV/s). For CTB dose–inhibition curves, plateau currents of glycine responses recorded with CTB were related to control plateaus. Open-channel diameters were derived from the relative permeabilities of a series of test anions (Cl^-, HCO_3^-, $HCOO^-$, and CH_3COO^-) as detailed (8). Voltage-clamp recordings from *Xenopus* oocytes injected with GlyR or nAcChoR complementary RNAs (cRNAs) were performed as described (22). Neither oocytes nor HEK-293 cells showed endogenous glycine responses in the range of the glycine concentrations used. The sodium salt of CTB was purchased from Alfa Chemie (Karlsruhe, Germany) and TPMP bromide was from Sigma.

RESULTS

CTB Block of Recombinant GlyR Channels. The application of glycine to HEK-293 cells transfected with the human GlyR α1-subunit cDNA elicits whole-cell Cl^- currents up to several nanoamperes (Fig. 2*A Left*). To test the effect of CTB on GlyR channel function, we coapplied 40 μM glycine with 20 μM CTB. This resulted in a rapid decline of the initial peak

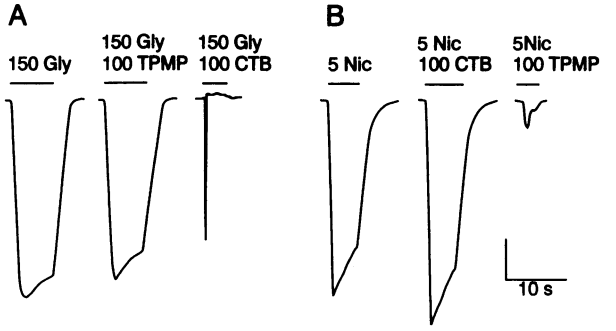

FIG. 4. Differential ability of CTB and TPMP to block anion-selective GlyR and cation-selective nAcChoR channels. The recordings were obtained from oocytes expressing the α1 GlyR (*A*) or the αβγδ nAcChoR (*B*). The numbers above the application bars indicate drug concentrations in μM, and the vertical scale bar corresponds to 250 nA (*A*) or 150 nA (*B*). (*A*) Glycine-induced currents were strongly blocked by CTB but not by TPMP. (*B*) Nicotine (Nic) responses were resistant to CTB but almost completely abolished by TPMP.

current to baseline levels (Fig. 2*A Center*). This effect was reversible, as glycine responses similar to control were recovered after a 2-min wash-out period (Fig. 2*A Right*). The persistence of the initial peak of the glycine response even at high concentrations of CTB suggested that the agonist-activated open state of the GlyR channel is the target of CTB's antagonistic action. Further, the extent of channel block by CTB, expressed as the percentage reduction of the plateau current by 1 μM CTB, increased with the glycine concentration coapplied (Fig. 2*B*). Thus, antagonism of GlyR channel function by CTB requires open channels.

To elucidate whether CTB interferes with glycine binding to the receptor, we recorded glycine dose–response curves in the absence and presence of CTB. Here, *Xenopus* oocytes injected with human α1-subunit cRNA were used because recordings from oocytes were much more stable than those from HEK-293 cells. The dose–response curves in Fig. 2*C* show that the effective glycine concentrations required for half-maximal plateau currents (EC_{50}) are roughly similar in the absence (270 μM glycine; see also ref. 22) and the presence (143 μM glycine) of 0.2 μM CTB. As the EC_{50} value for glycine should increase in the presence of a competitive antagonist, it appears that CTB exerts its blocking action in a way that is noncompetitive to glycine binding.

To investigate the voltage sensitivity of CTB block, we measured the *I–V* relationships of glycine-induced currents in α1 cDNA-transfected cells. With symmetrical chloride concentrations (145 mM) at both membrane faces, the *I–V* curves were linear, revealing a reversal potential of about 0 mV during the application of 50 μM glycine alone. In the presence of 1 μM CTB, glycine-induced currents were significantly smaller at positive as compared with negative membrane potentials (Fig. 3). This inward rectification indicates that the efficacy of CTB increases with membrane potential, a behavior expected for a negatively charged molecule blocking the channel from the outside of the cell.

Glycine responses of HEK-293 cells or oocytes expressing the GlyR α1 subunit were not significantly blocked by TPMP—a molecule that is structurally similar to CTB albeit positively charged (see Fig. 1)—at all concentrations tested (up to 20 μM in HEK-293 cells and to 100 μM in oocytes, Fig. 4*A*). Conversely, the application of 5 μM nicotine to oocytes expressing nAcChoR channels of the αβγδ type from rat muscle (23) elicited cationic currents, which were efficiently blocked by 100 μM TPMP but were insensitive to 100 μM CTB (Fig. 4*B*).

Subunit-Specificity of CTB Block. The dose-dependence of CTB block of different GlyR isoforms was investigated by using glycine concentrations corresponding to the EC_{50} values determined for each isoform (Table 1). Fig. 5 shows glycine responses recorded with increasing CTB concentrations. A CTB concentration causing half-maximal inhibition of plateau currents (IC_{50}) of 2.6 ± 0.7 μM (mean ± SD, n = 6 cells) was obtained for α1 homooligomers with 40 μM glycine. This value decreased to 1.3 ± 1.0 μM (n = 8) with 50 μM glycine in accordance with the observed use dependence of CTB block (Fig. 5*D*). Frequently, the initial peak currents in the presence of low CTB concentrations exceeded those of the control glycine response; a similar phenomenon has been observed for the TPMP block of the nAcChoR (24). In contrast to α1 homooligomers, α2 channels proved largely insensitive even at the highest CTB concentration used (IC_{50} >> 20 μM, n = 6; Fig. 5 *B* and *D*). Coexpressing α and β subunits in HEK-293 cells at an excess of β-subunit cDNA leads to the almost exclusive formation of functional α/β heterooligomers (7, 15). The CTB sensitivity of α1/β receptors (IC_{50} = 2.8 ± 2.5 μM, n = 6) was indistinguishable from that of α1 homooligomers. For α2/β channels, however, the IC_{50} value (7.5 ± 2.0 μM, n = 5) was lower than that of α2 homooligomers (Table 1). Hill coefficients for inhibition of glycine-induced currents by CTB were close to unity, indicating a single-site mechanism, which is expected for open-channel block (Table 1).

A Residue Within Transmembrane Segment M2 Determines the CTB Sensitivity of α Homooligomeric GlyRs. The channel-lining M2 segments of α1 and α2 subunits differ in only one amino acid position (7): Gly-254 of α1 is exchanged for an alanine in the α2 subunit (Fig. 5*E*). To examine the relevance of this substitution for the observed subunit specificity of CTB, we determined the sensitivity of mutant α1 G254A. Indeed, inhibition of glycine-induced currents by 20 μM CTB was negligible with this mutant (Fig. 5*C*), and the dose–inhibition curve (Fig. 5*D*) shows that this mutation strongly reduced CTB sensitivity (IC_{50} >> 20 μM, n = 5)—i.e., α1 G254A channels behave like α2 receptors. This suggests that the M2 segment of the α1 subunit constitutes the binding site

Table 1. Glycine activation and CTB block of recombinant glycine receptors

Receptor	Glycine EC_{50}, μM	Pore diameter, Å	CTB block		
			$[Gly]^t$, μM	IC_{50}, μM	Hill coeff.
α1	39 ± 17 (22)	5.34	40	2.6 ± 0.7 (6)	0.9 ± 0.2
			50	1.3 ± 1.0 (8)	1.0 ± 0.2
α2	84 ± 32 (7)	5.31	90	>> 20 (6)	ND
α1/β	48 ± 17 (29)	5.22	50	2.8 ± 2.5 (6)	1.1 ± 0.1
α2/β	95 ± 34 (6)	5.44	100	7.5 ± 2.0 (5)	0.9 ± 0.2
α1 G254A	14 ± 4 (6)	ND	10	>> 20 (5)	ND
α2/βB G278A	112 ± 31 (5)	ND	100	3.0 ± 1.6 (5)	0.9 ± 0.2

EC_{50} values ± SD were derived from the fits of dose–response curves. The number of cells, n, is in brackets; values for α1 and α1/β receptors are those of Bormann *et al.* (7). IC_{50} values ± SD (n cells) and the Hill coefficients (coeff.) ± SD for the CTB block are given together with the test glycine concentrations ($[Gly]^t$), which correspond to the individual EC_{50} values. (ND, not determined).

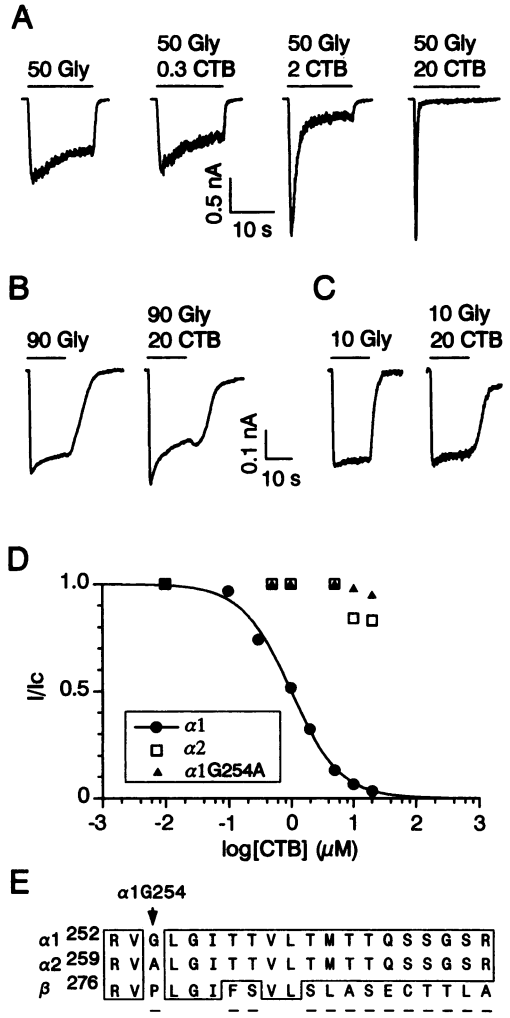

FIG. 5. Subunit-specific block of GlyR isoforms by CTB. (*A*) Inhibition of glycine-induced plateau currents of the α1 homooligomeric GlyR by increasing CTB concentrations. (*B*) Resistance of α2 GlyR toward 20 μM CTB. (*C*) Resistance of the mutant α1 G254A toward 20 μM CTB. Bars denote periods of drug application (15 s), and numbers correspond to the concentrations of the applied drugs in μM. The glycine concentrations applied are close to the EC_{50} values of the different GlyR isoforms (Table 1). (*D*) CTB dose dependence of the GlyR isoforms shown in *A–C*. Glycine-induced plateau currents were normalized to the control currents obtained in the absence of CTB. The sigmoidal curve shown for the α1 subunit is a fit to the equation $I/I_c = IC_{50}^n/(C^n + IC_{50}^n)$, where I/I_c represents normalized current, C the CTB concentration, and n the Hill coefficient. For the CTB-insensitive α2 (□) and α1 G254A receptors (▲), the data points were not fitted. (*E*) Sequence alignment of GlyR α1, α2, and β subunit M2 segments. Conserved residues are boxed, and the dashed line indicates the amino acids exchanged in the β subunit to generate mutant βB G278A.

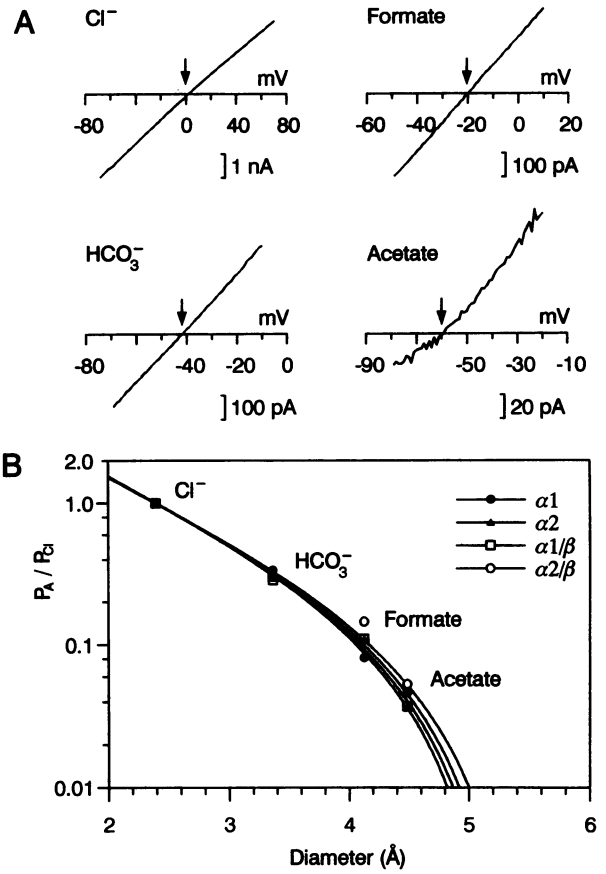

FIG. 6. Pore diameters of recombinant GlyR isoforms. (*A*) Reversal potential measurements of glycine-induced whole-cell currents from four different cells expressing the α1 subunit upon replacement of 140 mM internal Cl^- by various monovalent anions. The reversal potentials determined from the *x*-axis intercepts (arrows) of the I–V curves were 1 mV (Cl^-), −20 mV ($HCOO^-$), −42 mV (HCO_3^-), and −60 mV (CH_3COO^-). (*B*) Relation between relative permeability and apparent ionic diameter for the different GlyR isoforms. The permeability ratios (P_A/P_{Cl}) were calculated for the permeability of various test anions (P_A) relative to Cl^- permeability (P_{Cl}) from biionic reversal-potential measurements as shown in *A*. Ionic diameters were derived from limiting conductances of the ions. The data points were fitted with a model assuming spherical ions and with the permeability depending on ionic diameter and frictional forces in the channels (see ref. 8). From the fits, the estimated pore diameters are 5.34 Å for α1 (●), 5.31 Å for α2 (△), 5.22 Å for α1/β (□), and 5.44 Å for 2α/β (○).

for the blocker. In an analogous approach, we made a chimeric construct where the M2 segment of the β subunit was replaced by that of the α2 subunit (mutant βB G278A, Fig. 5*E*). However, upon coexpression of this chimera with the α2 subunit, which generates heterooligomers containing only M2 segments of the α2 type, the CTB resistance characteristic for α2 homooligomers was not seen (IC_{50} = 3.0 ± 1.6 μM, n = 5; Table 1). This suggests that transmembrane segments other than M2 may also contribute to the CTB sensitivity of α/β heterooligomeric GlyRs.

CTB Block and Pore Size. To assess whether the differential sensitivity of the various GlyR isoforms originates from different open-channel diameters, these were estimated from the relative permeabilities of a series of test ions of different sizes. However, the reversal potentials measured with Cl^-, $HCOO^-$, HCO_3^-, and CH_3COO^- under biionic conditions revealed similar correlations of permeability with anion size for all GlyR isoforms analyzed (Fig. 6). The model used to fit the decrease of permeability with ionic size (Fig. 6*B*) predicts the pores intrinsic to recombinant GlyRs to be of diameters (5.22–5.44 Å; Table 1) comparable to that of native GlyR in cultured spinal neurons (5.2 Å; ref. 8). Thus, the subunit specificity of CTB block is not related to the pore diameter of GlyR channels.

DISCUSSION

Our results demonstrate that CTB, a molecule not previously known to interact with channel proteins, potently and reversibly blocks the Cl^- channel of recombinant GlyR isoforms. The block proved to be noncompetitive to glycine binding and sensitive to membrane potential. The degree of block increased with glycine concentration (i.e., with the open-state probability of the channel), suggesting use-

dependence of CTB block. Moreover, GABA-gated Cl^- channels in rat hippocampal neurons were also blocked by low micromolar concentrations of CTB (unpublished experiments). Thus, this drug may be a blocker of Cl^- channels gated by different agonists. Importantly, a large difference was observed between α1 and α2 homooligomeric GlyRs with respect to their blocker sensitivities. This difference is accounted for by a primary structure variation of the respective channel-forming transmembrane segment M2: the Gly-254 → Ala change within the α1-subunit M2 segment completely abolished CTB sensitivity. These data qualify CTB as a subtype-specific open-channel blocker of the GlyR interacting with the channel-forming segment M2.

Previously, we have shown that the α1-subunit Gly-254 → Ala mutation converts the repertoire of elementary conductance states from α1 to that of α2 or α3 homooligomers (7). The equivalent position is of prime importance for other ligand-gated ion channels, too: (*i*) this position corresponds to the most constricted site, the "central ring," of the nAcChoR channel (4–6); and (*ii*) mutating this position confers resistance of insect $GABA_A$Rs to picrotoxinin and cyclodiene insecticides (25).

The negatively charged CTB molecule was found to be ineffective at the cation-selective nAcChoR. On the other hand, anion-selective GlyR channels were insensitive to the structurally similar but positively charged TPMP, which is known to block cationic currents through the nAcChoR (ref. 26 and this study). This indicates that the electric charge of a blocker molecule is an important determinant of its specificity and suggests an interaction with an electrostatic field inside the pore.

The isoform specificity of CTB may qualify this compound as a tool to probe the subunit structure of native GlyRs. This is of importance, as the expression of different GlyR subtypes is developmentally and spatially regulated in the mammalian central nervous system (10, 27).

We thank A. Herbold and G. Heiss-Herzberger for excellent technical assistance, Dr. V. Witzemann for kindly providing nAChoR cRNAs, Dr. R. Taylor for critically reading the manuscript, and Maren Baier for secretarial assistance. This work was supported by the Deutsche Forschungsgemeinschaft (SFB 169, Leibniz Programm) and the Fonds der Chemischen Industrie.

1. Langosch, D., Becker, C.-M. & Betz, H. (1990) *Eur. J. Biochem.* **194,** 1–8.
2. Unwin, N. (1993) *Neuron* **72,** 31–41.
3. Imoto, K., Busch, C., Sakmann, B., Mishina, M., Konno, T., Nakai, J., Bujo, H., Mori, Y., Fukuda, K. & Numa, S. (1988) *Nature (London)* **335,** 645–648.
4. Imoto, K., Konno, T., Nakai, J., Wang, F., Mishina, M. & Numa, S. (1991) *FEBS Lett.* **289,** 193–200.
5. Cohen, B. N., Labarca, C., Davidson, N. & Lester, H. A. (1992) *J. Gen. Physiol.* **100,** 373–400.
6. Villaroel, A., Herlitze, S., Koenen, M. & Sakmann, B. (1991) *Proc. R. Soc. London B* **243,** 69–74.
7. Bormann, J., Rundström, N., Betz, H. & Langosch, D. (1993) *EMBO J.* **12,** 3729–3737.
8. Bormann, J., Hamill, O. P. & Sakmann, B. (1987) *J. Physiol. (London)* **385,** 243–286.
9. Takahashi, T., Momiyama, A., Hirai, K., Hishinuma, A. & Akagi, H. (1992) *Neuron* **9,** 1155–1161.
10. Becker, C.-M., Hoch, W. & Betz, H. (1988) *EMBO J.* **7,** 3717–3726.
11. Hille, B. (1992) *Ionic Channels of Excitable Membranes* (Sinauer, Sunderland, MA).
12. Hucho, F. L., Oberthür, W. & Lottspeich, F. (1986) *FEBS Lett.* **205,** 137–142.
13. Revah, F., Galzi, J.-L., Giraudat, J., Haumont, P.-Y., Lederer, F. & Changeux, J.-P. (1990) *Proc. Natl. Acad. Sci. USA* **87,** 4675–4679.
14. Charnet, P., Labarca, C., Leonard, R. J., Vogelaar, N. J., Czyzyk, L., Gouin, A., Davidson, N. & Lester, H. A. (1990) *Neuron* **2,** 87–95.
15. Pribilla, I., Takagi, T., Langosch, D., Bormann, J. & Betz, H. (1992) *EMBO J.* **11,** 4305–4311.
16. Chen, C. & Okayama, H. (1987) *Mol. Cell. Biol.* **7,** 2745–2751.
17. Grenningloh, G., Schmieden, V., Schofield, P. R., Seeburg, P. H., Siddique, T., Mohandas, T. K., Becker, C.-M. & Betz, H. (1990) *EMBO J.* **9,** 771–776.
18. Grenningloh, G., Pribilla, I., Prior, P., Multhaup, G., Beyreuther, K., Taleb, O. & Betz, H. (1990) *Neuron* **4,** 963–970.
19. Gorman, C. M., Gies, C. R. & McCray, G. (1990) *DNA Protein Eng. Tech.* **2,** 3–10.
20. Hamill, O. P., Marty, A., Neher, E., Sakmann, B. & Sigworth, F. J. (1981) *Pflügers Arch.* **391,** 85–100.
21. Bormann, J. (1992) in *Practical Electrophysiological Methods*, eds. Kettenmann, H. & Grantyn, R. (Wiley–Liss, New York), pp. 136–140.
22. Schmieden, V., Grenningloh, G., Schofield, P. R. & Betz, H. (1989) *EMBO J.* **8,** 695–700.
23. Witzemann, V., Stein, E., Barg, B., Konno, T., Koenen, M., Kues, W., Criado, M., Hofmann, M. & Sakmann, B. (1990) *Eur. J. Biochem.* **194,** 437–448.
24. Spivak, C. E. & Albuquerque, E. X. (1985) *Mol. Pharmacol.* **27,** 246–255.
25. ffrench-Constant, R. H., Rocheleau, T. A., Steichen, J. C. & Chalmers, A. E. (1993) *Nature (London)* **363,** 449–451.
26. Lauffer, L. & Hucho, F. (1982) *Proc. Natl. Acad. Sci. USA* **79,** 2406–2409.
27. Malosio, M.-L., Marquèze-Pouey, B., Kuhse, J. & Betz, H. (1991) *EMBO J.* **10,** 2401–2409.